Hindawi
Advances in Materials Science and Engineering
Volume 2023, Article ID 9803294, 1 page
https://doi.org/10.1155/2023/9803294

Retraction

Retracted: Effect of SiC Particle Incorporated Dielectric Medium on Electrical Discharge Machining Behavior of AA6061/B4Cp/SiCp AMCs

Advances in Materials Science and Engineering

Received 6 April 2023; Accepted 6 April 2023; Published 19 April 2023

Advances in Materials Science and Engineering has retracted the article titled "Effect of SiC Particle Incorporated Dielectric Medium on Electrical Discharge Machining Behavior of AA6061/B4Cp/SiCp AMCs" [1] due to significant overlap with a previously published article by different authors [2].

References

[1] J. Khajuria, N. Nagabhooshanam, P. Sharma et al., "Effect of SiC Particle Incorporated Dielectric Medium on Electrical Discharge Machining Behavior of AA6061/B4Cp/SiCp AMCs," *Advances in Materials Science and Engineering*, vol. 2022, Article ID 2661158, 9 pages, 2022.

[2] S. G. Iyyappan, R. Sudhakarapandian, and M. Sakthivel, "Influence of silicon carbide mixed used engine oil dielectric fluid on EDM characteristics of AA7075/SiCp/B4Cp hybrid composites," *Materials Research Express*, vol. 8, no. 8, 2021.

Hindawi
Advances in Materials Science and Engineering
Volume 2022, Article ID 2661158, 9 pages
https://doi.org/10.1155/2022/2661158

Research Article

Effect of SiC Particle Incorporated Dielectric Medium on Electrical Discharge Machining Behavior of AA6061/B4Cp/SiCp AMCs

Johny Khajuria,[1] N. Nagabhooshanam,[2] Pankaj Sharma,[3] Atul Kumar,[4] Santosh Kumar Sahu,[5] Peyyala Sree Devi,[2] and Kuma Gowwomsa Erko [6]

[1]*Department of Mechanical Engineering, Mahant Bachittar Singh College of Engineering and Technology, Jammu, Jammu and Kashmir, India*
[2]*Department of Mechanical Engineering, Aditya Engineering College, ADB Road, Aditya Nagar, Surampalem 533437, Andhra Pradesh, India*
[3]*Department of Mechanical Engineering, JECRC University, Jaipur, India*
[4]*Department of Mechanical Engineering, SET, Mody University of Science and Technology, Lakshmangarh, Sikar 332311, Rajasthan, India*
[5]*Department of Mechanical Engineering, Veer Surendra Sai University of Technology, Burla 768018, Odisha, India*
[6]*Department of Mechanical Engineering, Ambo University, Ambo, Ethiopia*

Correspondence should be addressed to Kuma Gowwomsa Erko; kuma.gowwomsa@ambou.edu.et

Received 1 May 2022; Accepted 8 June 2022; Published 21 July 2022

Academic Editor: K. Raja

In this work, it was observed that using motor oil as the dielectric fluid when producing AA6061/SiCp/B4Cp hybrid composites provided wealth from waste. In these studies, modifications in silicon carbide (SiC) concentration, electrode (copper and brass), current, pulse time, and reinforcing weight percentage were tested. Surface roughness and machined hardness are measured and reported for each removed piece of the material. The bridging effect of silicon carbide particles raised the material removal rate (MRR), while a thorough dielectric fluid flush enhanced the Ra value. On the machined topography, the oil carbon content left dark smudges. Machining performance is superior to that of copper electrode-processed specimens. The MRR, TWR, and Ra all rise as the discharge current and pulse duration increase. Because there is no remelted layer, composites with low machining surface hardness had better finishes. The parameters were optimized using the TOPSIS approach, and it was observed that the efficiency of machining was enhanced by utilizing engine oil by the concentration of 4 gl^{-1}. Moreover, during machining, optimized parameters like pulse on time 36 seconds, current 4 Amps, and also a brass electrode.

1. Introduction

Standard machining methods were useless in composite materials because of the occurrence of strengthening elements [1]. EDM and other unconventional methods of machining are frequently used to attain high precision and accuracy. The key aims of the EDM are MRR, TWR, and Ra. Process variables such as electrical current, pulse on time, and tool material are all significant in determining machining characteristics [2, 3]. Machine tools can be made from a variety of materials, including copper, brass, graphite, Cu-W, and ZiC. The correct tool and workpiece combination must be determined to optimise machining performance [4–6]. It is possible to increase machine output by mixing foreign particles into the dielectric fluid [7].

There have been several research altering the particle size, powder materials, and powder concentration [8]. Powders including SiC, B_4C, Al_2O_3, and graphite are commonly used in PMEDM. Adding powder particles, according to the majority of findings, reduces the gap growth

and thus raises MRR [9–11]. Because of the homogeneous distribution of discharge energy, an improvement in MRR was attained. Short circuits are formed when powder particles are added above the limit, resulting in a significant decrease in MRR. Hong et al. [12] tested the kerosene dielectric by adding chromium powder to it. Results show that the addition of chromium powder to dielectric fluid raises material removal rate and surface roughness by 45 and 68%. Abdudeen et al. [13] investigated the dielectric fluid breakdown using powders for four distinct materials. The breakdown of dielectric was reduced when the concentration of powder was increased [14–16].

In terms of dielectric fluids, hydrocarbon, vegetable, and synthetic oil-based fluids are maximum and frequently used [13, 17]. Dielectric fluids such as kerosine, EDM oil, and deionized water are the most common. Machined by these traditional fluids, poisonous gas is released into the environment [18–20]. HSS-M35 was machined using argon, nitrogen, and air as dielectric media by [21]. Nitrogen and argon gas was found to be the finest dielectric medium for removing more material and producing the highest surface quality. Imran et al. [22] used distilled water and paraffin oil as dielectric media to manufacture AA6061 aluminium alloy. Using purified H_2O as dielectric resulted in a thicker white coating than using paraffin oil. Larger globules and surface pitting have been noticed under paraffin medium, according to the report as well [23–25].

Dielectric fluid properties of Jatropha biodiesel were examined by [26]. If you compare it to synthetic EDM oil, it performs better than kerosine in terms of machining, but it performs worse than kerosine in terms of cutting. Pure water and kerosine can be used as the dielectric medium to mill high-carbon and high-chromium steel, according to [27–29]. In this machining method, copper, graphite, and brass tools were employed, and the current and pulse duration were both dynamically modified. Carbon was thought to be deposited on the surface of machines that were operated in kerosene environment [30]. When specimens were fabricated in distilled water using a graphite tool, the MRR was larger and the Ra was lower. Deionized tap water was employed by the authors of [31] as an electric discharge medium. A decrease in surface quality was found as a result of machining that resulted in craters. Dielectric fluid made from multiwall carbon nanotubes and mixed with Kusum edible oil by the authors of [32] was utilized by them to manufacture EN-31.

The multicriteria decision-making (MCDM) technique is used in TOPSIS to be preferred because they resemble the deal scenario [33, 34]. When it came to solving a material election problem, TOPSIS was one of the most effective MCDM techniques. Finding the top solution and the nastiest solution yielded the top and worst values [35]. Finding these two perfect values led to the discovery of the optimum parameters. Four separate process parameters were varied by their EDM experiments [36]. The TOPSIS technique was used to discover the ideal process parameters for abrasive water jet machining and powder mixing to electric discharge drilling [37, 38]. Numerous studies using a variety of dielectric fluids and powders in combination with electric discharge machining have been published, according to scientific research [39–41]. There has never been any research on unused engine oil as a dielectric fluid. These projects sought to make money from waste by using engine oil as dielectric fluid for EDM on AA6061 hybrid composites [42].

Table 1: Chemical composition of AA6061.

Zn	Mn	Cu	Mg	Fe	Al
0.24	0.85	0.24	0.92	0.04	Remaining

2. Materials and Methods

The matrix material was AA6061, which is employed in the fabrication of aerospace structural parts because of its weldability and dimensional stability, and it is excellent for a wide range of diverse uses. Its element percentage is shown in Table 1. An average particle size of 5 μm was chosen as strengthening for the SiC and B4C materials. Modified stir casting was used to create the composite. In a graphite receptacle, the alloy was heated to 850°C. At 1000 rpm, the mixture is agitated for 180 seconds after injecting preheated SiC and B4C particles. Before reheating the composition to 850°C, the same was cooled to 420°C for 120 seconds and violently agitated. Engineering composites of various weight percentages have been made using the same method for releasing the charge into the preheated die steel. Figure 1 shows a schematic view of the electrical discharge machine.

The dielectric was made up of copper and brass, with different concentrations of SiC powder (0, 4, and 8 gl^{-1}) added to improve the machining properties. Table 2 depicts the dielectric characteristics of the used engine oil obtained from the automotive exhibition room. A mechanical stirrer, submersible flushing pump, and a 12-liter tank make up the PMEDM tank [43]. The variables' ranges were determined through preliminary tests. We assumed that all of our studies would display a steady discharge. Table 3 depicts the values of the input variables. Several responses are recorded, including MRR, TWR, Ra, and surface hardness (SH). For each trial, the machining time was set at 10 minutes. The specimen Ra was determined using an SJR210 surface roughness tester, which measured it 10 times and averaged the results. The Rockwell hardness testing machine was used to evaluate the surface hardness value following machining in accordance with ASTM standard E18. The TOPSIS (Technique for Order of Preference by Similarity to Ideal Solution), a multicriteria decision analysis optimization method, was used to discover the ideal process parameter value as follows:

$$\text{material removal rate} = (W_b - W_a), \tag{1}$$

$$\text{tool wear rate} = (T_b - T_a). \tag{2}$$

3. Results and Discussion

When powder concentration is 4 gl^{-1}, the MRR increased, and when it was 8 gl^{-1}, the MRR decreased. Particles suspended in a space between a tool and its workpiece will

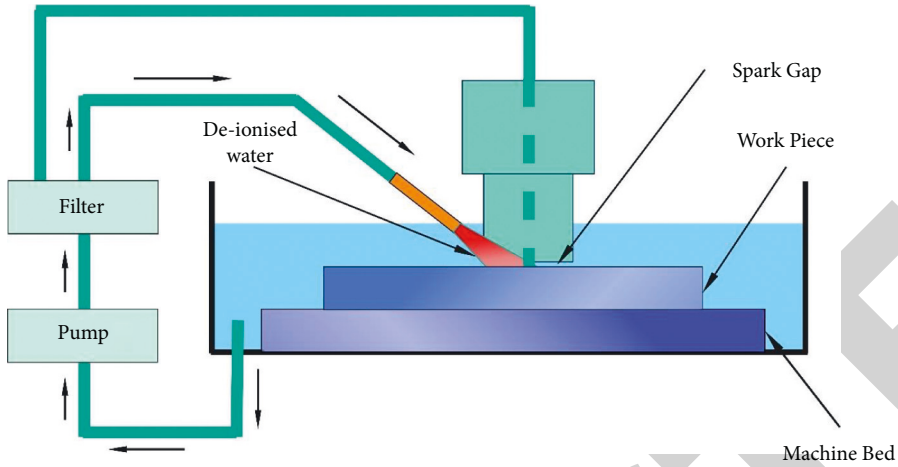

Figure 1: Schematic view of the electrical discharge machine.

Table 2: Dielectric fluid properties.

Property	Electrical discharge machining oil	Engine oil after used	Remarks
Strength (KVA)	47	65	Strength raises the efficiency of machining
Colour	Clear	Black	The workpiece is invisible
Carbon (%)	9	97	Black dot deposition on the surface of the machine due to carbon content
Flashpoint (oC)	>93	188	Enhancing the safety of work by higher flash point
Thermal conductivity ($Wm^{-1}\ k^{-1}$)	0.114	0.140	Heat dissipation raises due to thermal conductivity
Density ($kg\ m^{-3}$)	830	876	Blushing expands the density
Viscosity at 45°C (mm^2/s)	2.46	2.5	Heat transfer raises due to low viscosity
Specific heat ($kJ\ kg^{-1}\ K^{-1}$)	2.12	1.824	Specific heat is less in used oil compared to EDM oil

Table 3: Levels of process parameters.

Parameter	Levels
Current	2, 4, 6 *A*
Electrode material	Copper, brass
Powder concentration	0, 4, 8 gl^{-1}
Pulse on time	12, 24, 36μs
Dielectric fluid	Used engine oil
Work piece	$AA6061/SiC/B_4C$
Voltage	32*V*
The weight percentage of composite	5, 10, 15 $wt.\%$

increase spark frequency and intensity if applied a voltage. As a result, the MRR will rise. Table 4 illustrates the results of the inquiry. The findings were in line with prior research. As the spark gap widened further, more heat was released due to an increase in powder concentration. Machining the workpiece was not possible due to insufficient heat generated, thereby decreasing the MRR. With copper electrodes, samples cut with brass tools had a lower MRR.

In addition, it was discovered that the current MRR climbed until a saddle point of 4 A, at that time began to fall again. MRR increased more rapidly because the current flowed through a denser plasma channel and had a higher intensity, which naturally rises as the current increases as shown in Figure 2. As current flows across the plasma channel, MRR lowers. For a current of 6 A, however, the MRR was larger when the powder concentration was 4 gl^{-1}. Plasma channels shrink and produce greater heat as spark gaps increase owing to powder addition, according to this theory. Because of this, melting and vaporization are accelerated, increasing MRR. MRR was maximum at a powder concentration of 4 gl^{-1}. According to the data, the MRR decreases as the weight % of strengthening particles increases.

Copper electrodes, as seen in Figure 3, have a lower TWR than brass electrodes. This decrease in TWR was nominally lower for electrodes with greater melting temperatures because of the material's physical characteristics. As a result, copper has a lower TWR than brass due to its higher melting point. TWR decreases until it reaches the saddle point of 4 gl^{-1} and then begins to rise again. From the result, TWR can easily reduce due to the bulk of the negative ions passing over the process gap. Short circuits develop by increasing the powder concentrations, resulting in a rise in TWR. Increased discharge current erodes a greater amount of electrode material, increasing TWR. Increasing the pulse-on-time causes a raise in spark energy and an increase tool wear rate as previously noted. At an outlet current of 2 A, a pulse on time of 15 s, and a concentration of powder of 4 gl^{-1}, TWR was determined to be modest. tolerable work ratio (TWR) is minimum for composites with 5 and 10%

Table 4: EDM experimental results of AA7075 hybrid composites.

S. no.	Tool	Concentration of the powder	Current	Pulse on time	% of weight	Material removal rate	Tool wear rate	Surface roughness	Hardness	Expected values			
										Material removal rate	Tool wear rate	Surface roughness	Hardness
1	Cu	0	2	12	5	292	59	4.35	94	300.9	52.9	4.8	89.6
2	Cu	0	4	24	10	342	72	4.4	97	321.6	69.9	5.1	94.7
3	Cu	0	6	36	15	343	83	5.30	103	346.6	78.4	5.9	101.8
4	Cu	4	2	12	10	332	44	2.12	89	367.3	49.1	2.6	88.3
5	Cu	4	4	24	15	403	63	3.60	97	393.8	60.7	3.7	93.4
6	Cu	4	6	36	5	507	71	3.66	84	488.4	79.6	3.7	85.1
7	Cu	6	2	12	10	393	69	4.72	91	374.5	64.6	4.8	86.9
8	Cu	6	4	24	15	334	76	5.12	95	346.8	69.6	5.2	97.9
9	Cu	6	6	36	5	294	69	4.84	99	275.6	66.7	5.1	98.5
10	Br	0	2	12	5	297	83	5.67	96	292.7	87.7	5.7	97.3
11	Br	0	4	24	10	325	86	3.82	93	306.9	85.7	4.1	91.2
12	Br	0	6	36	15	395	88	4.29	97	302.4	87.7	4.9	94.0
13	Br	4	2	12	15	327	68	2.51	90	336.1	67.9	2.6	89.4
14	Br	4	4	24	5	443	74	1.73	85	469.1	74.5	1.4	85.7
15	Br	4	6	36	10	352	73	2.14	95	356.3	68.9	2.4	91.5
16	Br	6	2	12	10	379	79	3.98	95	356.9	78.5	4.4	94.0
17	Br	6	4	24	15	284	84	3.92	96	292.3	79.3	4.3	97.6
18	Br	6	6	36	5	304	77	4.17	91	307.8	72.4	4.6	89.9

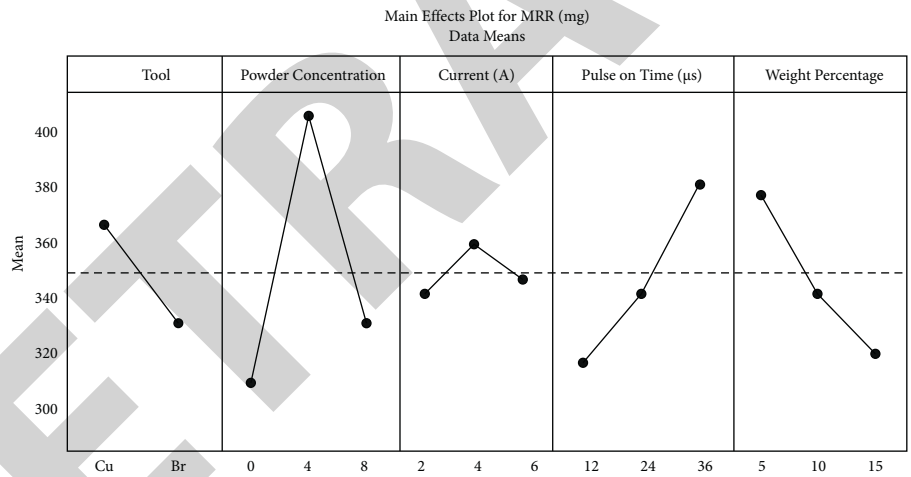

Figure 2: Differences in MRR concerning diverse process parameters.

reinforcing particles, but it rapidly rises when samples with 15% reinforcing particles are machined.

Figure 4 shows that the addition of SiC powder to the dielectric phase considerably reduces Ra. The distance separating the electrode and the workpiece widens as the particles are added. There are no more "globules" or "layers" of remelted material to be formed, which helps to increase the Ra of the gap. As a result of the increased strength of the powder, the gap distance grows even further, which reduces heat generation. As a result, the quality of the surface is lowered because of the production of voids and microcracks. A greater Ra value is created as the discharge strength is raised, and the surface is creating pits. The even distribution of discharge energy provided by $4\,gl^{-1}$ particles results in a finer surface finish. Because of the greater spark bombardment caused by the longer pulse-on-time, the surface's Ra value increased. Composites have a deteriorating surface quality with increasing weight fractions. Micropits emerge on the surface when reinforcing substances are removed from the surface during machining, which is consistent with prior observations.

Hardness values before machining ranged from 86, 93 to 97 HRB for composites containing 5, 10, and 15% reinforcing particles. A higher weight percentage led to higher hardness readings because of the presence of hard ceramic fragments. Machining composites with powder particles at $4\,gl^{-1}$ results in a loss of hardness as shown in Figure 5. The surface quality is raised by a more significant spark gap generated by the silicon carbide particles, reducing the production of remelted layers. The machined surface's hardness changes when reinforcing particles are removed from the surface.

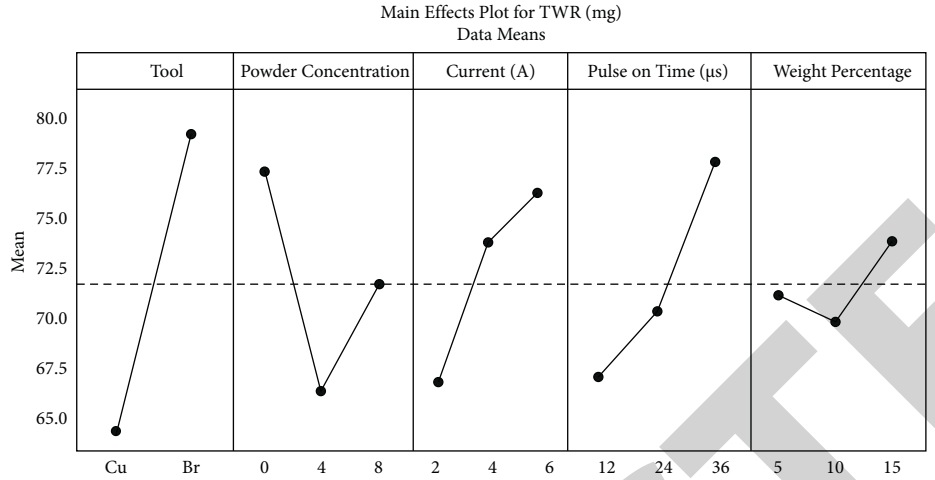

Figure 3: Differences in tool wear rate with respect to diverse process parameters.

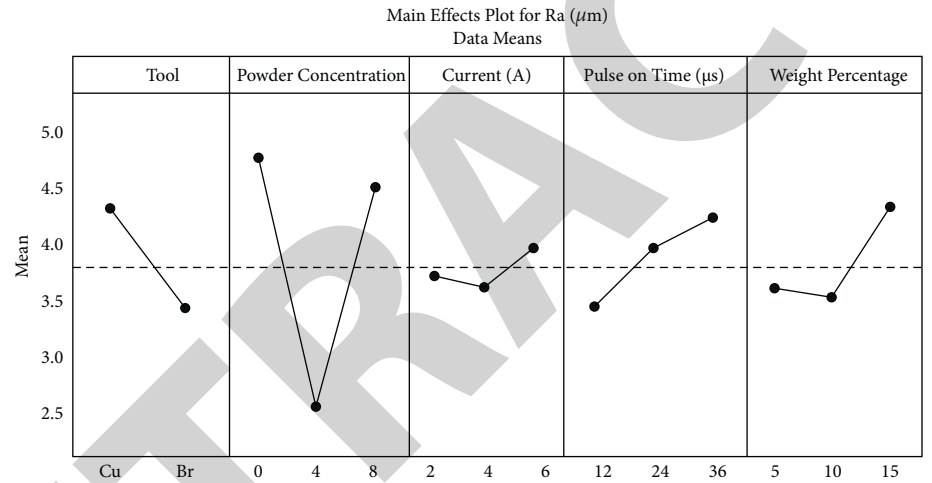

Figure 4: Differences in the roughness of surface with respect to diverse process parameters.

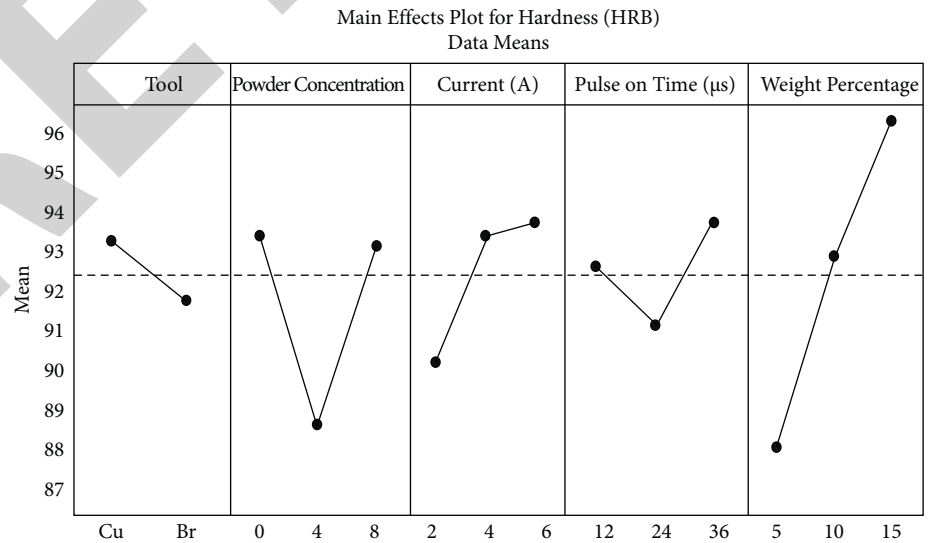

Figure 5: Differences in machined surface hardness concerning diverse process parameters.

Table 5: Enhanced values in investigational data set and technique for the order of preference by similarity to ideal solution.

Normalized matrix			Normalized decision matrix by weight			P^+	P^-	Pi	Rank
0.19321	0.78654	0.264558	0.06453	0.063454	0.12586	0.08	0.05	0.42	17
0.21674	0.228765	0.294875	0.08548	0.067416	0.11256	0.09	0.04	0.33	8
0.21724	0.264324	0.318748	0.08570	0.087124	0.125763	0.10	0.03	0.22	13
0.26340	0.168304	0.129588	0.09423	0.057861	0.053475	0.04	0.10	0.80	5
0.28243	0.199345	0.216590	0.10182	0.067543	0.187602	0.06	0.07	0.63	2
0.35346	0.257528	0.219147	0.12416	0.085197	0.183560	0.06	0.08	0.64	6
0.26107	0.218765	0.287365	0.096628	0.073482	0.112316	0.08	0.05	0.41	14
0.23103	0.241685	0.306361	0.083819	0.079502	0.116834	0.09	0.04	0.28	10
0.20223	0.221349	0.288545	0.073868	0.074356	0.116234	0.09	0.04	0.32	16
0.21260	0.296812	0.234585	0.076524	0.096557	0.131249	0.11	0.02	0.10	15
0.22523	0.283912	0.228826	0.081735	0.092867	0.082546	0.08	0.05	0.42	18
0.20234	0.306544	0.256510	0.075196	0.099688	0.101227	0.09	0.04	0.31	9
0.22657	0.238453	0.153482	0.082169	0.072830	0.063824	0.06	0.08	0.64	3
0.31124	0.261287	0.114098	0.108210	0.086154	0.149146	0.04	0.10	0.80	4
0.24321	0.231496	0.132034	0.087769	0.078526	0.092416	0.05	0.09	0.71	1
0.26015	0.237889	0.238608	0.093565	0.087409	0.084341	0.07	0.05	0.47	12
0.19796	0.272347	0.234812	0.072767	0.089825	0.099683	0.09	0.05	0.39	7
0.20167	0.248721	0.249612	0.076314	0.085153	0.094216	0.08	0.05	0.38	11
Wt.			0.43	0.4	0.4				
Eigen values			0.124268	0.058753	0.048523				
			0.072768	0.098769	0.131249				

Remelted layers are formed when the powder is added to composites while they are being machined, which makes the globules less stable. As a result of the high pulse on time, most of the molten material is deposited again on the surface due to insufficient flushing. Adding SiC particles to the dielectric fluid remedied this issue by increasing the spark gap and allowing for adequate flushing. The experimental data used in the prediction calculation was used to determine the regression coefficients of the second-order equation. This study indicated that the difference between actual and projected results was less than five percent.

4. Surface Topography

The occurrence of carbon in wasted engine oil had discovered to be the cause of black patches on the composite surface. Due to the irregular spreading of discharge energy, a significant fracture was detected on the surface; the acquired data are exactly matched to the experimental data, as shown in the Figure 5. It is possible to discern globules, remelted layers, and deeper pits all over the surface, all of which significantly impair the surface. The surface topography at a higher magnification of 2000x, reveals craters, tiny holes, and micropits. Because of this, the surface roughness value was increased by approximately 20 μm. Machined composites have a reduced hardness because they lack a remelted layer on the surface. The spark gap's surface quality improves because melting debris is washed away by the extra space between the electrode and the workpiece. Other researchers have made similar discoveries. There is an increase in the production of carbon black spots, fracturing, and pitting at higher magnifications. This is compensated for by a higher spark frequency. Thus, for fine-finish machining of hybrid composites, an increased spark gap was shown to be preferable.

4.1. TOPSIS. Due to identifying the optimum possible mixing of parameters, the Technique for Order of Preference by Similarity to the Ideal Solution (TOPSIS) optimization approach was applied. Because policymakers and end-users are both involved, this solution has an advantage. There were 18 experiments with three responses, thus a crucially in a matrix form of 18×3 has been produced as displayed in Table 4. As a first step, data sets are normalized by equations (3) and (4). The normalizing matrix is B_{ij}, where i denotes the number of experiments and j is the number of responses. As a result, these normalized matrices were used to generate a weighted normalized judgment matrix C_{ij} as follows:

$$Bij = \frac{Aij}{\sum \sqrt{()}}, \tag{3}$$

$$Cij = wj * Bij. \tag{4}$$

To calculate eigen values, the weighted normalized decision matrix is weighted, with $£^+$ being the highest value and $£^-$ being the lowest value in equation (5). According to formula (6), for nonbeneficiary qualities, the calculation was reversed.

For beneficiaries,

$$£^+ = \text{Max}\,(\text{Cij})_{i=1}^{n},\ £^- = \text{Min}\,(\text{Cij})_{i=1}^{n}. \tag{5}$$

For nonbeneficiaries,

$$£^+ = \text{Min}_{i=1}^{n},\ £^- = \text{Max}\,(\text{Cij})_{i=1}^{n}. \tag{6}$$

Using this equation, we were able to determine the optimal P^+ and ideal in the nastiest P^- solutions in equation (7). According to equation (8) indicated in Table 5, the dispersion between ideal and nonideal is determined.

$$(P^+, P^-) = \sum \sqrt{(\text{Cij} - \pounds^+)^2 + (\text{Cij} - \pounds^n)^2}, \quad (7)$$

$$O^i = \left(\frac{P^-}{P^+ + P^-}\right). \quad (8)$$

It was discovered that the discharge current of 4 A and also pulse on time of 45 μs were the ideal parametric values when the electrode was brass and the powder mixture concentration was 4 gl^{-1}.

5. Conclusion

Hybrid composites were successfully fabricated using AA6061/SiCp/B4Cp and dielectric fluid based on motor oil. A range of variables, including dielectric powder concentration, pulse time, and electrode material, was used to analyze machining performance. Following research, the following conclusion was reached:

(1) The bridging activity of SiC particles increased spark frequency and energy strength, improving MRR. When an amount is applied beyond the saddle point, short circuit occurs. Brass-tool manufactured specimens exhibited the highest MRR when compared to copper-tool manufactured specimens. This raises the MRR by increasing discharge current and pulse on time, which increases plasma channel density and spark energy.

(2) With the increased spark gap, the flushing of dielectric fluid enhances surface quality when suspended SiC particles are present. Due to bombardment and surface blitzkrieg, the Ra value raises with raising pulse on time and current. When increased beyond the threshold, this results in reduced heat generation and the formation of voids and pits.

(3) Its higher melting point makes it possible for the copper electrode to have a more efficient total work rate (TWR). SiC particles reduce TWR by reducing the mobility of negatively charged ions across the gap. TWR rises in proportion to longer pulse on times and higher discharge currents.

(4) The mechanical characteristics of composites are adversely affected by increases in wt.% of reinforcing elements. In terms of machining surface hardness, remelted layer and globule formation have a greater impact than normal. Higher surface quality can be achieved with lower machined hardness specimens.

(5) Carbon in the used engine oil causes a black spot on the machined surface. Surface features such as pits, remelted layers, crater valleys, and globules were apparent. Adding SiC particles reduce surface roughness by preventing the creation of the remelted layer. The surface quality deteriorates when the length of the crater valley is extended by SiCp at a concentration of 6 gl^{-1}.

(6) The TOPSIS optimization technique is used to optimize the input variables. Current, 6 amps; pulse on time, 45 μs; and brass tool are the best process variables for the machining of AA6061/SiCp/B_4Cp underutilized engine oil dielectric medium.

Data Availability

The data used to support the findings of this study are included within the article. Further dataset or information is available from the corresponding author upon request.

Conflicts of Interest

The authors declare that there are no conflicts of interest regarding the publication of this paper.

Acknowledgments

The authors appreciate the support from Ambo University, Ethiopia, for the research and preparation of the manuscript. The authors appreciate the support from the Veer Surendra Sai University of Technology, Aditya College of Engineering, and JECRC University for the assistance in completing this work.

References

[1] P. Sivaprakasam, J. Udaya Prakash, P. Hariharan, and S. Gowri, "Micro-electric discharge machining (Micro-EDM) of aluminium alloy and aluminium matrix composites - a review," *Advances in Materials and Processing Technologies*, vol. 2021, pp. 1–16, 2021.

[2] T. Sathish, V. Mohanavel, K. Ansari et al., "Synthesis and characterization of mechanical properties and wire cut EDM process parameters analysis in AZ61 magnesium alloy + B4C + SiC," *Materials*, vol. 14, no. 13, p. 3689, 2021.

[3] M. U. Gaikwad, A. Krishnamoorthy, and V. S. Jatti, "Investigation and optimization of process parameters in electrical discharge machining (EDM) process for NiTi 60 Mater," *Res. Express*, vol. 6, Article ID 6065707, 2019.

[4] K. Mausam, K. Sharma, G. Bharadwaj, and R. P. Singh, "Multi-objective optimization design of die-sinking electric discharge machine (EDM) machining parameter for CNT-reinforced carbon fibre nanocomposite using grey relational analysis," *Journal of the Brazilian Society of Mechanical Sciences and Engineering*, vol. 41, pp. 1–8, 2019.

[5] R. Ranjith, P. Tamilselvam, T. Prakash, and C. Chinnasamy, "Examinations concerning the electric discharge machining of AZ91/5B4CP composites utilizing distinctive electrode materials," *Materials and Manufacturing Processes*, vol. 34, no. 10, pp. 1120–1128, 2019.

[6] D. Purusothaman, R. S. Suresh Kumar, and B. G. Sivakumar, "Optimization of process parameter in machining inconel 800 by electrical spark eroding machine," *Journal of Chemical and Pharmaceutical Sciences*, vol. 9, no. 2, pp. 974–977, 2016.

[7] H. K. Kansal, S. Singh, and P. Kumar, "Technology and research developments in powder mixed electric discharge machining (PMEDM)," *Journal of Materials Processing Technology*, vol. 184, no. 1-3, pp. 32–41, 2007.

[8] A. Y. Joshi and A. Y. Joshi, "A systematic review on powder mixed electrical discharge machining," *Heliyon*, vol. 5, pp. 1–12, Article ID e02963, 2019.

[9] G. Talla, S. Gangopadhayay, and C. Biswas, "State of the art in powder-mixed electric discharge machining: a review,"

Proceedings of the Institution of Mechanical Engineers - Part B: Journal of Engineering Manufacture, vol. 231, no. 14, pp. 2511–2526, 2017.

[10] S. Tripathy and D. K. Tripathy, "Optimization of process parameters and investigation on surface characteristics during EDM and powder mixed EDM," *Innovative Design and Development Practices in Aerospace and Automotive Engineering*, Springer, Singapore, pp. 385–391, 2017.

[11] M. C. Nguyen, L. A. Tung, B. T. Danh et al., "Influence of input factors on material removal rate in PMEDM cylindrical shaped parts with silicon carbide powder suspended dielectric," *Key Engineering Materials*, Trans Tech Publications Ltd, vol. 861, , pp. 129–135, 2020.

[12] T. T. Hong, N. V. Cuong, B. T. Danh et al., "Multi-Objective optimization of PMEDM process of 90CrSi alloy steel for minimum electrode wear rate and maximum material removal rate with silicon carbide powder," *Materials Science Forum*, Trans Tech Publications Ltd, vol. 1018, , pp. 51–58, 2021.

[13] A. Abdudeen, J. E. Abu Qudeiri, A. Kareem, T. Ahammed, and A. Ziout, "Recent Advances and Perceptive Insights into Powder-Mixed Dielectric Fluid of EDM," *Micromachines*, vol. 11, Article ID 11754, 2020.

[14] A. P. Tiwary, B. B. Pradhan, and B. Bhattacharyya, "Influence of various metal powder mixed dielectric on micro-EDM characteristics of Ti-6Al-4V Mater," *Manuf. Processes*, vol. 34, 2019.

[15] S. S. Kumar, T. Varol, A. Canakci, S. T. Kumaran, and M. Uthayakumar, "A review on the performance of the materials by surface modification through EDM," *Int. J. Lightweight Mater. Manuf*, vol. 4, 2021.

[16] N. A. J. Hosni and M. A. Lajis, "Experimental investigation and economic analysis of surfactant (Span-20) in powder mixed electrical discharge machining (PMEDM) of AISI D2 hardened steel," *Machining Science and Technology*, vol. 24, no. 3, pp. 398–424, 2020.

[17] S. Jeavudeen, H. S. Jailani, and M. Murugan, "Powder additives influence on dielectric strength of EDM fluid and material removal," *International Journal of Machining and Machinability of Materials*, vol. 22, no. 1, pp. 47–61, 2020.

[18] J. E. A. Qudeiri, A. Zaiout, A. H. I. Mourad, M. H. Abidi, and A. Elkaseer, "Principles and characteristics of different EDM processes in machining tool and die steels SNAppl," *Science*, vol. 2020, Article ID 102082, 2020.

[19] X. Li, D. Wei, Q. Li, and X. Yang, "Study on effects of electrode material and dielectric medium on arc plasma in electrical discharge machining," *International Journal of Advanced Manufacturing Technology*, vol. 107, no. 11-12, pp. 4403–4413, 2020.

[20] B. Singaravel, K. C. Shekar, G. G. Reddy, and S. Deva Prasad, "Performance Analysis of Vegetable Oil as Dielectric Fluid in Electric Discharge Machining Process of Inconel 800 Mater," *Sci. Forum 97877-83*, Trans Tech Publications Ltd, vol. 978, , 2020.

[21] S. Fattahi and H. Baseri, "Analysis of dry electrical discharge machining in different dielectric mediums," *Proceedings of the Institution of Mechanical Engineers - Part E: Journal of Process Mechanical Engineering*, vol. 231, no. 3, pp. 497–512, 2017.

[22] M. Imran, S. M. Rahmanshah, S. Mehmood, and R. Arshad, "EDM of aluminum alloy 6061 using graphite electrode using paraffin oil and distilled water as dielectric medium," *Adv. Sci. Technol. Research*, vol. 11, 2017.

[23] M. Yunus Khan, P. Sudhakar Rao, and B. S. Pabla, "Investigations on the feasibility of Jatropha curcas oil based biodiesel for sustainable dielectric fluid in EDM process," *Materials Today Proceedings*, vol. 26, pp. 335–340, 2020.

[24] M. Patel GowdruChandrashekarappa, S. Kumar, D. Y. Pimenov, and K. Giasin, "Experimental Analysis and Optimization of EDM Parameters on HcHcr Steel in Context with Different Electrodes and Dielectric Fluids Using Hybrid Taguchi-Based PCA-Utility and CRITIC-Utility Approaches," *Metals*, vol. 2021, Article ID 11419, 2021.

[25] T. Muthuramalingam, "Effect of diluted dielectric medium on spark energy in green EDM process using TGRA approach," *Journal of Cleaner Production*, vol. 238, Article ID 117894, 2019.

[26] R. Bajaj, A. R. Dixit, and A. K. Tiwari, "Machining performance enhancement of powder mixed electric discharge machining using Green dielectric fluid," *Journal of the Brazilian Society of Mechanical Sciences and Engineering*, vol. 42, pp. 1–20, 2020.

[27] S. H. Mousavi-Nasab and A. Sotoudeh-Anvari, "A Comprehensive MCDM-Based Approach Using TOPSIS, COPRAS and DEA as an Auxiliary Tool for Material Selection Problems," *Materials & Design*, vol. 121, 2017.

[28] V. S. Viswanth, R. Ramanujam, and G. Rajyalakshmi, "Performance study of eco-friendly dielectric in EDM of AISI 2507 super duplex steel using Taguchi-fuzzy TOPSIS approach," *International Journal of Productivity and Quality Management*, vol. 29, no. 4, pp. 518–541, 2020.

[29] R. Nadda, R. Kumar, T. Singh, R. Chauhan, A. Patnaik, and B. Gangil, "Experimental investigation and optimization of cobalt bonded tungsten carbide composite by hybrid AHP-TOPSIS approach," *Alexandria Engineering Journal*, vol. 57, no. 4, pp. 3419–3428, 2018.

[30] J. Jayaraj, R. Sundaresan, and S. Chinnamuthu, "Multi-criteria decision of W-powder mixed electro discharge drilling parameters using TOPSIS approach," *Mechanics*, vol. 25, pp. 52–56, 2019.

[31] N. Yuvaraj and M. Pradeep Kumar, "Multiresponse optimization of abrasive water jet cutting process parameters using TOPSIS approach Mater," *Manuf. Processes*, vol. 30, 2015.

[32] T. C. Wang and H. D. Lee, "Developing a fuzzy TOPSIS approach based on subjective weights and objective weights," *Expert Systems with Applications*, vol. 36, 2009.

[33] V. Tao Le, "The influence of additive powder on machinability and surface integrity of SKD61 steel by EDM process," *Materials and Manufacturing Processes*, vol. 36, no. 9, pp. 1084–1098, 2021.

[34] M. A. Razak, A. M. Abdul-Rani, A. A. Aliyu et al., "The potential of improving the Mg-alloy surface quality using powder mixed EDM," *Progress in Engineering Technology. Advanced Structured Materials*, Springer nature, Switzerland, pp. 43–53, 2019.

[35] P. N. Huu, "Study of the effects of process parameters on tool wear rate in powder mixed electrical discharge machining by Taguchi method," *Science and Technology Development Journal*, vol. 20, pp. 55–60, 2017.

[36] C. Prakash, H. K. Kansal, B. S. Pabla, and S. Puri, "Experimental investigations in powder mixed electric discharge machining of Ti35Nb – 7Ta – 5$Zr\beta$-titanium alloy Mater," *Manuf. Processes*, vol. 32, 2017.

[37] M. V. Chame, P. Swaminadhan, and M. S. Bembde, "Optimization of process parameters of powder mixed dielectric EDM for MRR and Ra," *Optimization*, vol. 4, pp. 1039–1041, 2017.

[38] K. Dhakar and A. Dvivedi, "Dry and near-dry electric discharge machining processes," *Materials Forming, Machining*

and Tribology, Springer International Publishing, Switzerland, pp. 249–266, 2017.

[39] S. K. Sahu, T. Jadam, S. Datta, and G. Nandi, "Effect of using SiC powder-added dielectric media during electro-discharge machining of Inconel 718 superalloys," *Journal of the Brazilian Society of Mechanical Sciences and Engineering*, vol. 40, 2018.

[40] R. Ranjith, P. K. Giridharan, C. Velmurugan, and C. Chinnusamy, "Formation of lubricated tribo layer, grain boundary precipitates, and white spots on titanium-coated graphite-reinforced hybrid composites," *Journal of the Australian Ceramic Society*, vol. 55, no. 3, pp. 645–655, 2019.

[41] R. Ranjith, P. K. Giridharan, and J. Devaraj, "INFLUENCE OF TITANIUM-COATED (B4C + SiC) PARTICLES ON ELECTRIC DISCHARGE MACHINING OF AA7050 HYBRID COMPOSITES," *High Temperature Material Processes An International Quarterly of High-Technology Plasma Processes*, vol. 20, no. 2, pp. 93–105, 2016.

[42] S. Ramesh, M. P. Jenarthanan, and B. K. As, "Experimental investigation of powder-mixed electric discharge machining of AISI P20 steel using different powders and tool materials Multidiscip," *Model. Mater. Struct.*vol. 14, pp. 549–566, 2018.

[43] I. Corny, J. Pitel, and S. Hasova, "Statistical Approach to Optimize the Process Parameters of HAZ of Tool Steel EN X32CrMoV12-28 after Die-Sinking EDM with SF-Cu Electrode," *Metals*, vol. 735, 2017.